Available online at www.sciencedirect.com

ScienceDirect

Journal of Nuclear Materials 374 (2008) 1–8

journal of nuclear materials

www.elsevier.com/locate/jnucmat

Evaluation of self-welding susceptibility of an austenitic stainless steel (alloy D9) in sodium

Hemant Kumar [a], S.K. Albert [a], V. Ramakrishnan [b], C. Meikandamurthy [b], G. Amarendra [c], A.K. Bhaduri [a,*]

[a] *Materials Joining Section, Materials Technology Division, Indira Gandhi Centre for Atomic Research, Kalpakkam 603102, India*

[b] *Sodium Facilities Division, Indira Gandhi Centre for Atomic Research, Kalpakkam 603102, India*

[c] *Material Science Division, Indira Gandhi Centre for Atomic Research, Kalpakkam 603102, India*

Received 14 September 2006; accepted 3 July 2007

Abstract

Self-welding susceptibility of a 15Cr–15Ni–2Mo titanium-modified austenitic stainless steel (alloy D9), in both annealed and 20% cold-worked conditions, have been evaluated in flowing sodium at 823 K for 2160 and 4320 h under contact stress of 9.4 MPa. Tests were performed on flat-on-flat geometry of hollow cylindrical specimens under compression. One pair of 20% cold-worked alloy D9 vs. 20% cold-worked alloy D9 specimens tested for 4320 h was self-welded for which the breakaway shear force was measured. Scanning electron micrographs of the self-welded region showed that portions of the original interface no longer existed. The paper discusses the experimental set-up installed in the sodium loop test facility and the results of self-welding susceptibility studies on this material.

1. Introduction

The design of the prototype fast breeder reactor (PFBR) involves bundles of fuel pins contained in hexagonal wrappers located in the reactor core. The material chosen for the hexagonal wrappers is a 15Cr–15Ni–2Mo Ti-modified austenitic stainless steel (alloy D9), which are arranged vertically in a close-packed array to provide a compact core. Liquid sodium, which is used as a coolant, flows through these ducts extracting heat from the core. Due to compact design of the core, the wrappers would be in contact with each other, and hence to localize the area of contact, pads are provided on the hexagonal wrappers. These pads are integral with the wrapper and constitute a projection on its outer surface at a specified location. Consequently, each wrapper could come in contact with the neighbouring wrapper at the location of these pads.

During reactor operation at about 823 K, the contact stress experienced by the wrapper pads could be approximately 8 MPa. The use of high purity sodium (with an oxygen content less than 3 ppm) in the reactor that renders the surfaces from oxide films, the high temperature and the presence of stress between the mating surfaces of the wrapper pads can lead to self-welding at the location of contact. This can in turn lead to seizure thereby making the removal of the fuel subassembly difficult, once it reaches desired burn-up of 100 GWd/ton. Thus, it is essential to evaluate the self-welding susceptibility of this material in flowing sodium at operating temperature so as to simulate the conditions as experienced during reactor operation.

Self-welding, also known as diffusion bonding or adhesion occurs when two smooth bodies are pressed against each other. When they are mated and crystals of the mating surfaces come in close contact, strong inter-atomic forces and weak inter-molecular forces of attraction come into play, promoting intense adhesion. This involves a sequence of stages: deformation of the surfaces in apparent contact due to loading thereby causing an increase in the actual

* Corresponding author.
E-mail address: bhaduri@igcar.gov.in (A.K. Bhaduri).

0022-3115/$ - see front matter
doi:10.1016/j.jnucmat.2007.07.003

area of contact, and then volumetric diffusion of atoms across contact interface followed by recrystallisation. These result in self-welding of the mating surfaces at the contact points of the asperities [1].

Self-welding susceptibility of different grades of austenitic stainless steels has been evaluated in sodium by different investigators. Studies carried out by Yokota and Shimoyashiki [2] on grades 304 and 321 austenitic stainless steel in sodium at 778–823 K under contact stresses of 12–98 MPa for 100–900 h showed that a significant breakaway shear force is required to separate self-welded specimens. Also, the self-welding coefficient (defined as the breakaway force by shear per unit contact pressure during testing) for similar material combinations was proportional to the square root of the contact period and increased with the sodium temperature. Self-welding tests by Agostini and Masetti [3] carried out for 1, 15 and 45 days on mill-finished samples made of 20% cold-worked AISI 316 stainless steel under a contact force of 530 N at sodium temperatures of 673 and 823 K, showed no evidence of self-welding. Based on studies by Huber and Mattes [4] on the influence of different self-welding parameters, such as contact area, contact pressure, surface roughness and contact time, on the breakaway shear force for self-welded 15Cr–15Ni–2Mo vs. 15Cr–15Ni–2Mo surfaces at 973 K, it was found that with increasing contact pressure and contact time, the breakaway shear force increased. Further, the breakaway shear force is higher for mating surfaces with smooth surface finish than with those having a rough surface finish.

This paper describes the experimental set-up for self-welding susceptibility tests on selected material combinations in flowing sodium, and discusses the results of this experimental work.

2. Experimental

As per the design of PFBR, the temperature and contact stress experienced by the wrapper pads during reactor operation are expected to be 823 K and 9.4 MPa. Hence, the self-welding susceptibility of alloy D9, in both the annealed and 20% cold-worked conditions, was evaluated under a contact stress of 9.4 MPa in reactor grade (oxygen content <3 ppm) flowing sodium at 823 K for dwell periods of 2160 and 4320 h which corresponds to duration of approximately 3 and 6 months, respectively. All other testing parameters were kept such that the actual reactor operating conditions were simulated.

The experimental set-up for self-welding susceptibility studies in flowing sodium was provided with an inner shaft, outer shell, load cell and provision for holding specimens at the bottom (Fig. 1). The contact pressure was applied by tightening the disc springs at the top. The whole experimental set-up was immersed in a cylindrical vessel in which liquid sodium flows at a temperature of 823 K. The purity of the sodium in the vessel was maintained by passing the sodium continuously through a purification system consisting of pre-filter and cold trap, with the cold trap being maintained at 396–406 K.

The specimens for self-welding susceptibility studies were hollow cylinders of 21.4 mm outer diameter, 15.8 mm inner diameter and 15 mm length. The top and bottom surfaces of these hollow cylindrical specimens were the mating surfaces for the test. These specimens were fabricated from alloy D9 rods in the annealed and 20% cold-worked conditions. The surface finish of the specimens was kept <2 μm, which was similar to that of the components. The chemical composition of the alloy D9 used is given in Table 1. The average room temperature hardness of the annealed and 20% cold-worked alloy D9 was measured as 130 and 231 VHN, respectively. The following combinations of annealed and 20% cold-worked alloy D9 were subjected to self-welding test in flowing sodium at 823 K under a contact stress of 9.4 MPa in two different test rigs for test durations of 2160 and 4320 h, respectively:

(i) Annealed alloy D9 vs. annealed alloy D9,
(ii) Annealed alloy D9 vs. 20% cold-worked alloy D9,
(iii) 20% cold-worked alloy D9 vs. 20% cold-worked alloy D9.

The specimens were assembled in the test fixture. A gap of 2–3 mm was maintained between the mating surfaces to enable flush of their surfaces with hot sodium before loading into the test vessel. Argon gas purging was employed to flush air out of the vessel, and then sodium was allowed into the vessel. After flushing the contact surfaces of the specimens with hot liquid sodium for 24 h, load was applied on the specimens by tightening disc springs at the top. The specimens were then kept under load for 2160 h. Similarly, specimens were loaded also into another test set-up for 4320 h. After completion of these tests, the disc springs were loosened to release the load, the specimens removed from the vessel, and sodium cleaning was done by alcohol.

Breakaway shear force required for the separation of the self-welded specimen pair was measured using the experimental set-up shown in Fig. 2. In this set-up, one of the specimens in the self-welded pair is held in a vice while the other one was pulled using a threaded rod to which a load cell was attached. The load recorded at the time of separation of the self-welded specimens was taken as the breakaway force. The specimen surfaces after separation were examined under scanning electron microscope. Energy dispersive spectroscopic (EDS) analysis of the location of self-welding as well as away from it were also carried out.

Microstructure of the specimens before and after self-welding susceptibility tests were examined using optical microscope. Auger electron spectroscopy (AES) was carried out on selected specimen surfaces to examine the effect of flowing sodium on the surface chemistry of the specimens.

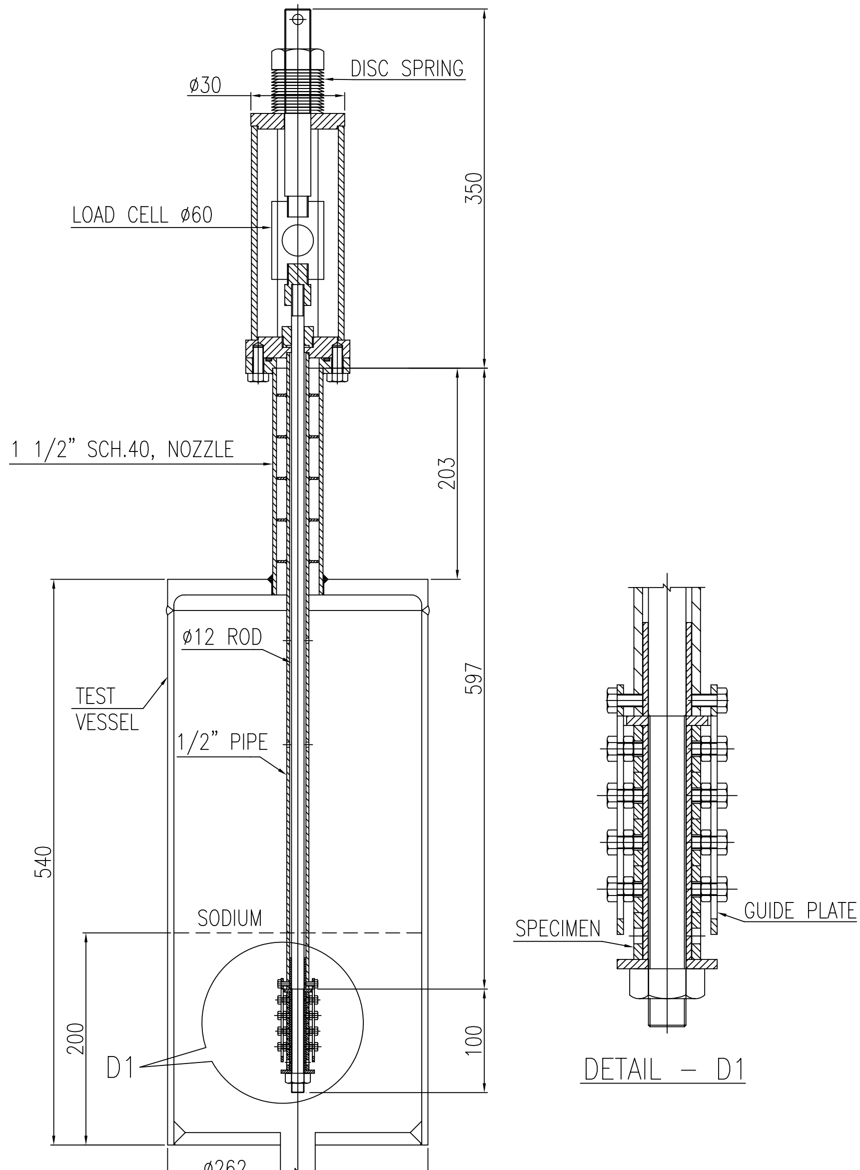

Fig. 1. Experimental set-up for self-welding susceptibility tests.

Table 1
Chemical composition of alloy D9 (in wt%)

Material	Ni	Cr	Mo	Mn	Si	Ti	C	P	S	N	Fe
Alloy D9	15.07	15.05	2.25	1.51	0.51	0.32	0.05	0.01	0.0025	66 ppm	Balance

Hardness of the specimens before and after the tests was measured using Vickers hardness tester at 5 kg load. Hardness profile from the specimen surface was taken using Vickers microhardness tester at 100 g load.

3. Results and discussion

No self-welding was observed in the 20% cold-worked alloy D9 specimens after testing for 2160 h. However, the annealed alloy D9 specimen pair showed some sticking of specimens, but the specimens got separated while cleaning with alcohol. The sticking observed could have been due to bonding of the sodium solidified in between the two specimens. After testing for 4320 h, no self-welding was observed in the annealed alloy D9 specimens, while self-welding occurred in one of the 20% cold-worked D9 specimen pairs. The results of self-welding test are summarised in Table 2. The breakaway shear force for the self-welded specimen pair was found to be 202 N.

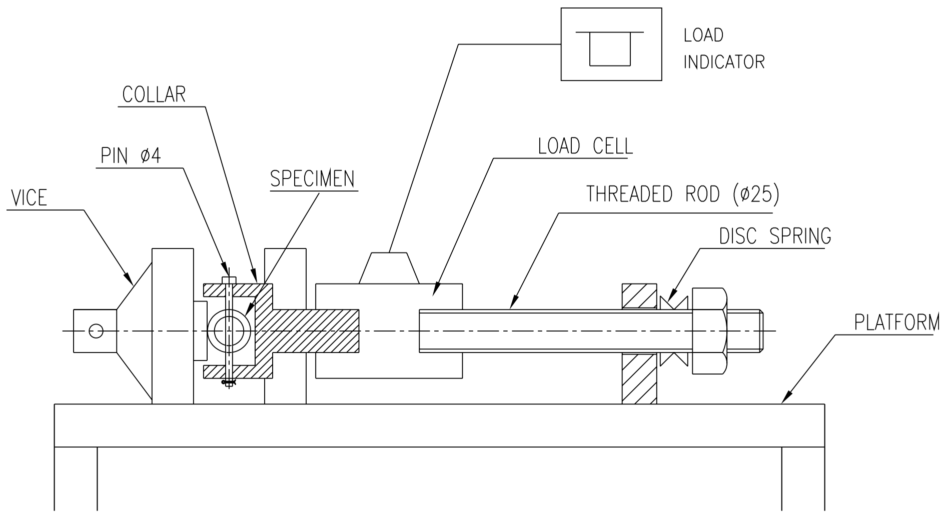

Fig. 2. Schematic set-up for measuring breakaway shear force of self-welded specimens.

Table 2
Self-welding behaviour of annealed and 20% cold-worked (CW) alloy D9 material combinations, with surface roughness of <2 μm, in reactor grade flowing sodium at 823 K under contact stress of 9.4 MPa

Material combinations	Dwell time (h)	Self-welding behaviour	No. of pairs tested	No. of pairs self-welded	Breakaway shear force (N)
20%CW D9 vs. 20%CW D9	2160	No self-welding	2	Nil	–
20%CW D9 vs. annealed D9	2160	No self-welding	1	Nil	–
Annealed D9 vs. annealed D9	2160	Minor adhesion	1	Nil	
20%CW D9 vs. 20%CW D9	4320	Self-welded	2	1	202
20%CW D9 vs. annealed D9	4320	No self-welding	1	Nil	–
Annealed D9 vs. annealed D9	4320	No self-welding	1	Nil	–

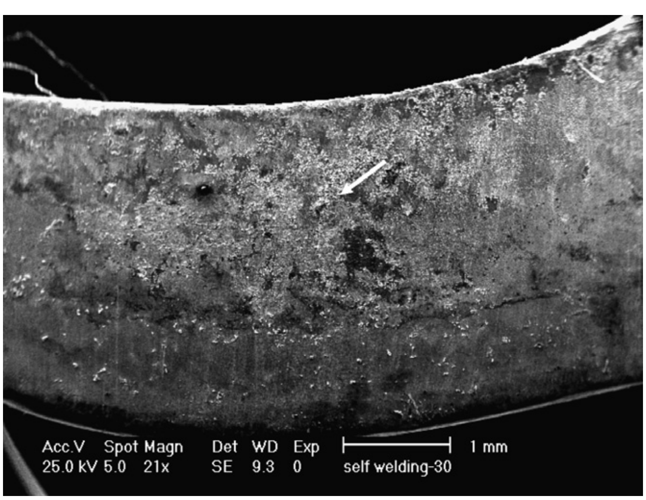

Fig. 3. SEM micrograph showing surface damage in self-welded region of 20% cold-worked specimen after testing for 4320 h in flowing sodium at 823 K.

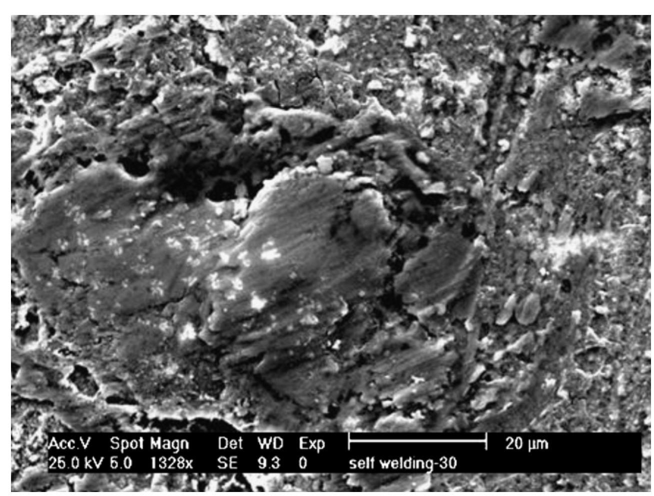

Fig. 4. SEM micrograph showing surface damage in self-welded region of 20% cold-worked specimen after testing for 4320 h in flowing sodium at 823 K.

SEM on self-welded 20% cold-worked alloy D9 specimens tested for 4320 h revealed significant surface damage as shown in Fig. 3. The entire mating surface was not self-welded, it had occurred only at a few locations on the surface. Fig. 4 shows the location of self-welding at higher magnification (as marked by arrow in Fig. 3) and this reveals the damage caused by separation. The results of EDS analysis at locations of self-welding and of no self-welding are shown in Figs. 5 and 6, respectively. Counts for sodium is low for self-welded locations indicating there

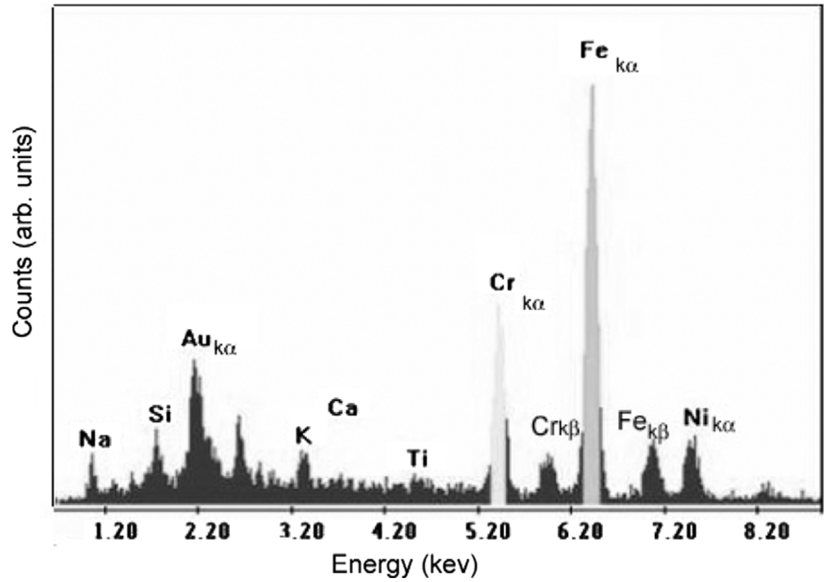

Fig. 5. Elemental counts by EDS in self-welded region of 20% cold-worked specimen after testing for 4320 h in flowing sodium at 823 K, showing low Na content.

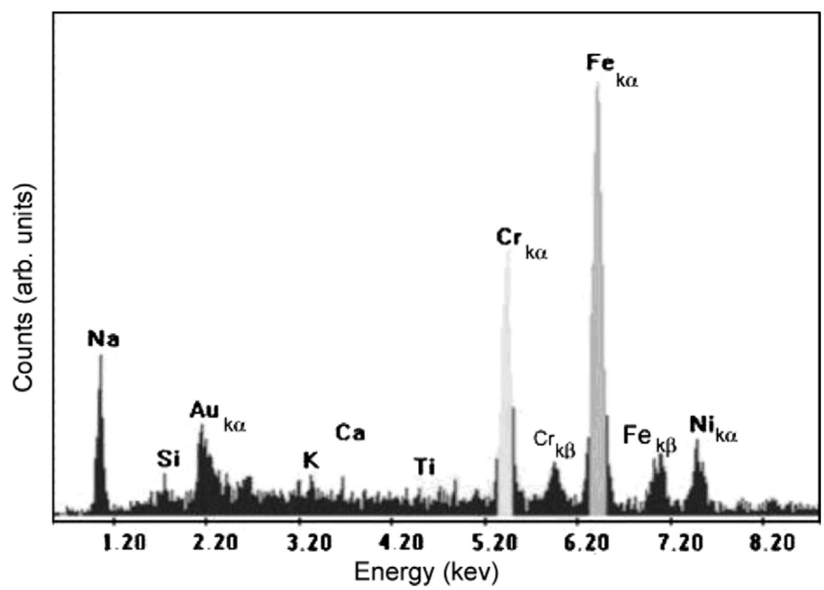

Fig. 6. Elemental counts by EDS in non self-welded region of 20% cold-worked specimen after testing for 4320 h in flowing sodium at 823 K, showing relatively high Na content.

was no interaction of sodium with the specimen surfaces at this location, once self-welding occurred.

Microstructures of the annealed and 20% cold-worked D9 alloy before test are shown in Figs. 7(a) and (b), respectively. Cold-worked microstructure reveals higher density of twins than the annealed microstructure. Figs. 8(a) and (b) shows the microstructures of the annealed specimens after 2160 h of testing, close to the specimen surface and ~0.5 mm away from it, respectively. A comparison of these microstructures reveals thicker grain boundaries near the surface than those away from it indicating precipitation along the grain boundaries near the surface. Microstructures from identical locations of 20% cold-worked specimens after same duration of testing are shown in Figs. 9(a) and (b), respectively. In this case too thickening of grain boundaries near the surface is observed; however, its extent is much lower than the annealed specimens.

Results of hardness measurements on annealed and 20% cold-worked specimens before and after self-welding test are given in Table 3. An increase in hardness with duration of testing is observed for both annealed and cold-worked specimens. This increase is more pronounced for annealed specimens than the cold-worked specimens. It is interesting to note that prolonged exposure to high temperature did not cause any reduction in hardness for cold-worked material. Microhardness profiles across the cross-section of an

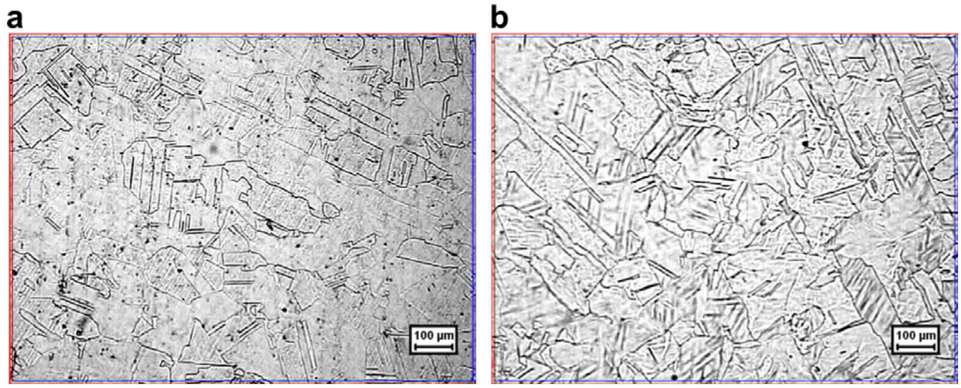

Fig. 7. Microstructure of alloy D9 material used for self-welding susceptibility studies: (a) in annealed condition; and (b) in 20% cold-worked condition.

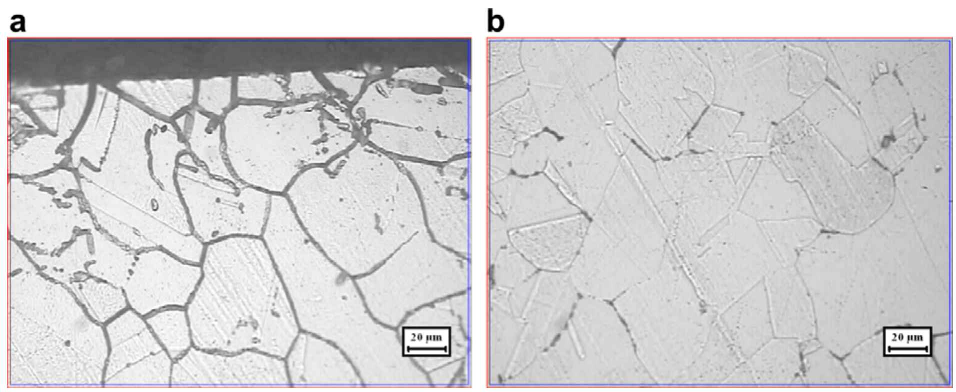

Fig. 8. Microstructure taken perpendicular to the mating surface of annealed alloy D9 specimen, after testing for 2160 h in flowing sodium at 823 K, for: (a) outer most layer of the specimen; (b) ∼0.5 mm away from outer most layer.

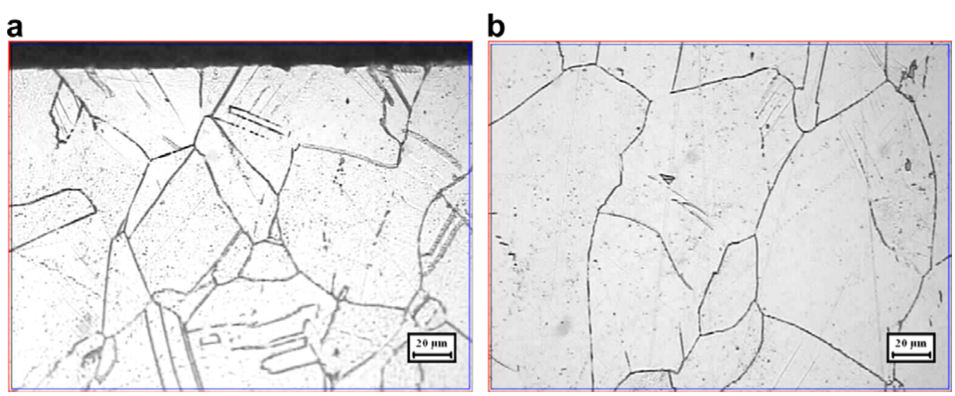

Fig. 9. Microstructure taken perpendicular to the mating surface of 20% cold-worked alloy D9 specimen, after testing for 2160 h in flowing sodium at 823 K, for: (a) outer most layer of the specimen; (b) ∼0.5 mm away from outer most layer.

annealed and 20% cold-worked specimens after 2160 h of testing are shown in Figs. 10 and 11, respectively. Specimens were cut along its length and these measurements were taken across its thickness at the middle portion. Hardness profile clearly shows an increase in hardness near the surface on either side (though more scatter is observed for cold-worked specimen) and this increase is more for the annealed specimen than the cold-worked one. Further, it is also observed that this increase in hardness is high on the outer side of the specimen than in the inner side.

Table 3
Hardness of annealed and 20% cold-worked (CW) alloy D9 specimens before and after self-welding tests

Materials	Vickers hardness (VHN)		
	Before test	After 2160 h test	After 4360 h test
Annealed D9 specimen	134	152	160
20%CW D9 specimen	238	246	250

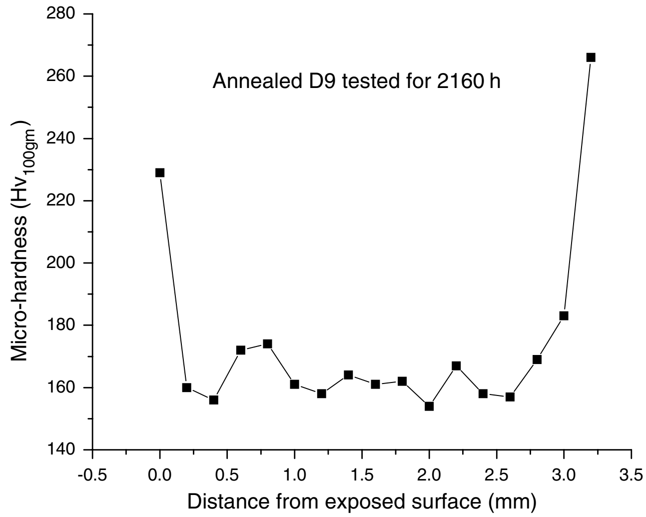

Fig. 10. Micro-hardness profile across cut cross-section of annealed alloy D9 specimen, after testing for 2160 h in flowing sodium at 823 K.

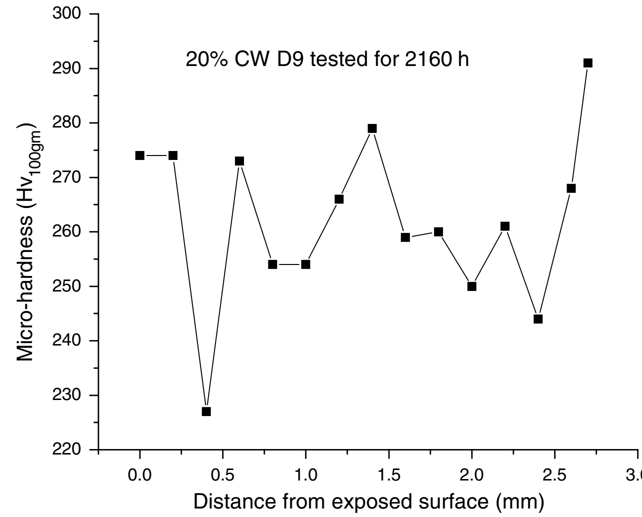

Fig. 11. Micro-hardness profile across cut cross-section of 20% cold-worked alloy D9 specimen, after testing for 2160 h in flowing sodium at 823 K.

AES spectra of a reference D9 specimen and that of specimens (annealed and 20% cold-worked) tested for 2160 h are shown in Fig. 12. Clear peaks of Fe, Cr, O, Ni, C are seen in reference sample while in exposed specimens, it is found that Fe, Cr peaks heights go down and there is an increase in C peak, indicating carburization on the surface of the exposed specimens. A comparison of the C peak for the sodium exposed specimens indicates more carbon in annealed D9 specimen surface than in the cold-worked specimen surface.

The above results clearly indicate that during testing, carburisation of the specimens have taken place. It can be concluded that precipitation observed along the grain boundary near the surface and high hardness levels close to surface are due to increase in carbon content near the surface. Since, tests are conducted in flowing sodium; difference in carbon activity between different components of the sodium loop would have caused this carbon pick up of the specimens. It should be noted that the carbon content in the sodium is maintained below 25 ppm.

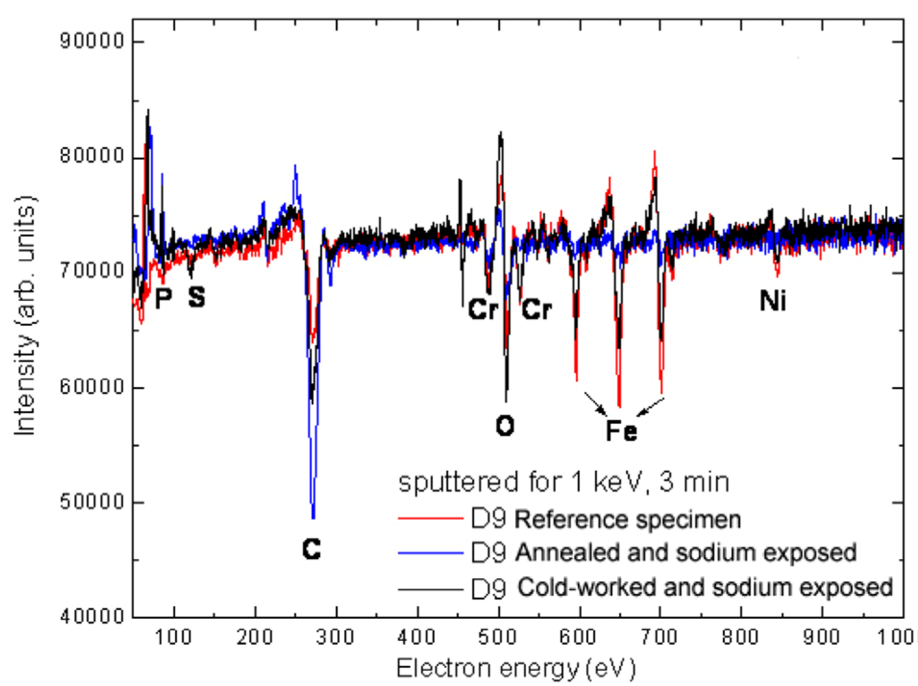

Fig. 12. AES spectra of reference D9, annealed D9 and 20% cold-worked D9 samples taken from 2160 h tests. Peaks due to various elements are marked. (All samples were given the same treatment prior to the measurements i.e., sputtered for 1 keV, 3 min after mounting inside the chamber to remove the surface contamination).

There appears to be a difference in the carbon pick up of annealed and cold-worked specimens. Microstructural evidence, hardness data and AES results all indicate that carbon pick up is more in annealed specimens than in the cold-worked specimens. An exact reason for this difference is not clear from this study. Further data on the effect of cold-work on carbon activity and carbon diffusion would be required for a suitable explanation of this phenomenon.

It shall be noted that while sodium exposure resulted in an increase in the surface hardness of the annealed D9 specimens (due to carbon pick up), change in hardness for cold-worked specimens was only marginal. It is quite possible that cold-worked material would have undergone some recovery and recrystallisation during prolonged exposure to high temperature. A comparison of the microstructure of the 20% cold-worked specimen before sodium exposure (Fig. 7(b)) with those after exposure (Fig. 9) reveals significant reduction in twin density, which suggests some recovery of the cold-worked structure has taken place. It appears that increase in hardness caused by carbon pick up has been partially nullified due to reduction in hardness caused by recovery.

The cold-work in the material can facilitate self-welding by promoting recovery and recrystallisation. The deformation experienced at the asperities of the mating surfaces of two specimens subjected to self-welding test, is augmented by the prior cold-work in the material. This would in turn increase the kinetics of recovery and recrystallisation at a given temperature. As recovery and recrystallisation takes place by diffusion, atoms diffuse across the asperities that are in contact which eventually results in self-welding. The higher is the time available for this diffusion, the more is the probability of self-welding. The facts the self-welding occurred only in tests of 4320 h duration (not in 2160 h test), that too only in one pair, and the breakaway forced required is quite low, indicate that even for the cold-worked D9 alloy, the susceptibility to self-welding is not very high.

4. Conclusions

(1) The experimental set-up designed to evaluate the susceptibility of material combinations to self-welding was successful in closely simulating the actual operating conditions.

(2) Self-welding susceptibility tests on eight pairs of three different combination (annealed D9 vs. annealed D9, annealed D9 vs. 20% cold-worked D9, and 20% cold-worked D9 vs. 20% cold-worked D9) under 9.4 MPa contact stress were carried out for 2160 and 4320 h in reactor grade flowing sodium at 823 K. There was no self-welding in any of the mating surfaces after 2160 h of testing. However, after 4360 h of testing, self-welding was observed in one of the two mating surfaces of 20% cold-worked D9 alloy. The breakaway force required to separate the self-welded specimen was 202 N.

(3) Exposure of the specimens to flowing sodium during testing resulted in carburisation of the specimen surfaces, which in turn caused an increase in the surface hardness of the specimens.

(4) Analysis of the results indicates that recovery and recrystallisation of the cold-worked structure would have contributed to the self-welding observed between the mating surfaces of 20% cold-worked D9 alloy.

Acknowledgements

The authors acknowledge the support and advice received from Dr S.K. Ray, Head of Materials Technology Division, Mr K.K. Rajan, Head of Sodium Facilities Division, as also from other members of the Sodium Facilities Division and Dr P. Parameswaran of Physical Metallurgy Section.

References

[1] S. Chander, C. Meikandamurthy, R.D. Kale, R. Krishnamurthy, Wear 162–164 (1993) 458.
[2] N. Yukota, S. Shimoyashiki, Nucl. Technol. 81 (1988) 407.
[3] P. Agostini, E. Masetti, Liquid Metals Technol. Energy Prod. 501 (1988) 1.
[4] F. Huber, K. MattesProc International Conference on Liquid Metals Technology in Energy Production, Champion, Pennsylvania USA, 1976.